Available online at www.sciencedirect.com
SCIENCE DIRECT
Journal of Molecular Catalysis A: Chemical 249 (2006) 211–217
JOURNAL OF MOLECULAR CATALYSIS A: CHEMICAL
www.elsevier.com/locate/molcata

Characterization and catalytic performance of TiO_2 nanotubes-supported gold and copper particles

Baolin Zhu, Qi Guo, Xueliang Huang, Shurong Wang, Shoumin Zhang, Shihua Wu, Weiping Huang *

Department of Chemistry, Nankai University, Tianjin 300071, PR China

Received 28 November 2005; received in revised form 7 January 2006; accepted 9 January 2006
Available online 21 February 2006

Abstract

TiO_2 nanotubes are prepared via the reaction of anatase TiO_2 powder with NaOH solution. Gold and gold–copper supported on TiO_2 nanotubes (Au/TiO_2 NTs and Au–Cu/TiO_2 NTs) are synthesized by deposition–precipitation method. The prepared materials are characterized with BET, powder X-ray diffraction (XRD), transmission electron microscopy (TEM) and high-resolution transmission electron microscopy (HRTEM). Their catalytic performance for low-temperature CO oxidation is studied by using a microreactor–GC system. The influence of support, pH of $HAuCl_4$ solution, calcination temperature and atmosphere as well as gold content on the catalytic performance of Au/TiO_2 NTs are investigated. Compared with Au/TiO_2 NTs, the catalytic performance of Au–Cu/TiO_2 NTs is better.

Keywords: Gold; Copper; Modified TiO_2 nanotubes; Catalytic performance; CO oxidation

1. Introduction

In recent decades, the catalytic oxidation of CO has become an important research topic due to its wide applications, e.g., elimination of CO from automobile emissions, CO gas sensors, gas purification in the laser and air-purification devices for respiratory protection [1–4]. Since the remarkable catalytic properties of supported gold nanoparticles for low-temperature CO oxidation was reported by Haruta et al. [5,6], many studies have been devoted to such kind of catalyst [7–10]. It is generally agreed that the catalytic activity of gold catalysts depends on the size of the gold particles, but the nature of the support material has also been suggested to play a key role [10–12]. Easily reducible oxides, such as TiO_2 [13–16], Fe_2O_3 [11,17–19], NiO [6,11], ZnO [20,21], CeO_2 [22,23] and Co_3O_4 [5,6,24], etc., might have cooperative effects with gold particles and can give rise to active catalysts for low-temperature CO oxidation. Being one of the most active catalysts, Au/TiO_2 system has been intensively researched [13–16]. Its catalytic activity is related to not only the size of gold particles but also the textural properties of support TiO_2, i.e., its propensity for facile adsorption and storage of oxygen [25,26]. TiO_2 nanotubes, which have large surface area, should be better support than TiO_2 powder for preparation of supported catalysts [27]. In 1998, Kasuga developed a simple hydrothermal process to prepare TiO_2 nanotubes of high quality [28]. The multilayer TiO_2 nanotubes have diameters of about 10 nm and large surface area [28,29]. However, gold-modified ones, which should exhibit good catalytic performance, are seldom reported [30–32]. We have prepared gold-modified TiO_2 nanotubes by using CTAB capped gold particles as gold precursor [32]. But the prepared catalyst has poor activity for CO oxidation because of the lack of active surface areas. In this paper, Au/TiO_2 NTs and Au–Cu/TiO_2 NTs are prepared by deposition–precipitation method. The effects of support, preparation conditions and gold content upon the catalytic activity of Au/TiO_2 NTs for CO oxidation are investigated. In order to reduce gold content and enhance the catalytic activity of Au/TiO_2 NTs, copper is added during the fabrication process.

2. Experimental

2.1. Preparation of samples

All of the chemicals are analytical grade and used without further purification. Raw TiO_2 powder is pure anatase crystal.

* Corresponding author. Tel.: +86 22 23502996; fax: +86 22 23502669.
E-mail address: huangw@eyou.com (W. Huang).

1381-1169/$ – see front matter © 2006 Elsevier B.V. All rights reserved.
doi:10.1016/j.molcata.2006.01.013

Its surface area and particle size are 10 m^2/g and 100 nm, respectively. Water is of ~18 MΩ cm resistivity.

2.1.1. Preparation of TiO_2 nanotubes

TiO_2 nanotubes are synthesized in a manner similar to that reported by Kasuga et al. [28]. Raw TiO_2 powder is dispersed in an aqueous solution of NaOH (10 M) and charged into a Teflon-lined autoclave. The autoclave is heated in an oil bath at 150 °C for 12 h. Prepared sample is washed with 0.1 M HCl solution and water, respectively. White powder is obtained after they are dried at 80 °C in air. Multilayer nanotubes of high quality can be observed with TEM. Their surface area is 428 m^2/g. The texture of TiO_2 nanotubes can withstand calcination below 400 °C [33].

2.1.2. Preparation of Au/TiO_2 NTs and gold-modified TiO_2 powder (Au/TiO_2 powder)

TiO_2 nanotubes are first dispersed in water and then an appropriate volume of $HAuCl_4$ solution (0.21 mg/ml) is added. The solution is adjusted to various pH with $NH_3{\cdot}H_2O$ and agitated for 1 h. Then the suspension is centrifuged and washed with water to remove Cl^- ions. After dried at 80 °C overnight, the precipitate is heated to decompose the Au(III) complexes into gold metal particles under various conditions. 2 wt.% Au/TiO_2 powder is prepared by a similar process for comparative study of different support.

2.1.3. Preparation of Au–Cu/TiO_2 NTs

TiO_2 nanotubes are dispersed in water and then $Cu(NO_3)_2$ solution is added. After water is evaporated completely at 100 °C under stirring, the impregnated TiO_2 nanotubes are calcined at 300 °C for 3 h and CuO supported on TiO_2 nanotubes (CuO/TiO_2 NTs) are obtained. The CuO/TiO_2 NTs instead of TiO_2 nanotubes are used as support to synthesize Au–Cu/TiO_2 NTs as process 2.1.2. The calculated gold and copper contents are 0.1 and 8 wt.%, respectively. CuO/TiO_2 NTs are reduced in hydrogen at 150 °C for 2 h to obtain TiO_2 nanotubes-supported copper (Cu/TiO_2 NTs) for comparative study.

2.2. Sample characterization

BET analysis is performed using an ASAP 2010 surface area and porosimetry analyzer. The powder X-ray diffraction (XRD) experiments are carried out at room temperature using a Rigaku D/Max-2500 X-ray diffractometer (Cu Kα $\lambda = 0.154$ nm) to identify crystal phase of the products. Diffraction peaks of crystalline phases are compared with those reported in the JCPDS Data File. The average crystalline size is calculated from the X-ray line broadening according to Scherrer equation [34]. TEM images are obtained with a Philips T20ST transmission electron microscopy working at 200 kV.

2.3. Catalytic activity

Catalytic performance of the samples is tested using a fixed bed flow microreactor (7 mm i.d.) under atmospheric pressure using 100 mg catalyst powder. Reaction gas mixture consisting of 1% CO balanced with air is passed through the catalyst bed at a total flow rate of 33.6 ml/min. The reactant and product composition is analyzed on-line with a GC-508A gas chromatograph equipped with a thermal conductivity detector (TCD). $T_{50\%}$ and $T_{100\%}$, which are important parameters for evaluating catalysts' performance, are the temperature for 50 and 100% CO conversion on catalyst, respectively.

Table 1 gives all characteristics of the prepared samples.

3. Results and discussion

3.1. Microstructural characterization of the modified TiO_2 nanotubes

Fig. 1 depicts the typical XRD patterns of all the catalysts. Diffractions that are attributable to anatase phase of TiO_2 crystal are clearly detectable in all materials (JCPDS 21-1272). Peak at $2\theta = 44°$ in Samples b, c, d, e, f and g can be filed to (2 0 0) plane of gold (JCPDS 4-0784), which proves that TiO_2 nanotubes are loaded with gold particles. However, no obvious gold peak is found in Samples a, h, i, j, k, l and m. The reasonable interpretation should be that the gold particles in them are too small to be detected by XRD. New peaks at $2\theta = 43°$ and 50° emerge in Sample m corresponding well to (1 1 1) and (2 0 0) diffractions of copper (JCPDS 4-836), respectively, which indicates that copper particles exist in Sample m.

The average gold particle sizes calculated from line broadening of (2 0 0) diffraction peak using Scherrer equation are listed in Table 1. It can be seen that average size of gold particles increases with the raise of solution pH and anneal temperature, which indicates that high pH and anneal temperature are mainly responsible for the agglomeration of gold particles. It has been reported that catalytic performance of supported gold catalysts depends markedly on the size of gold particles [10–12], and therefore exactly controlling experimental condition is indispensable for preparing Au/TiO_2 NTs with high activity.

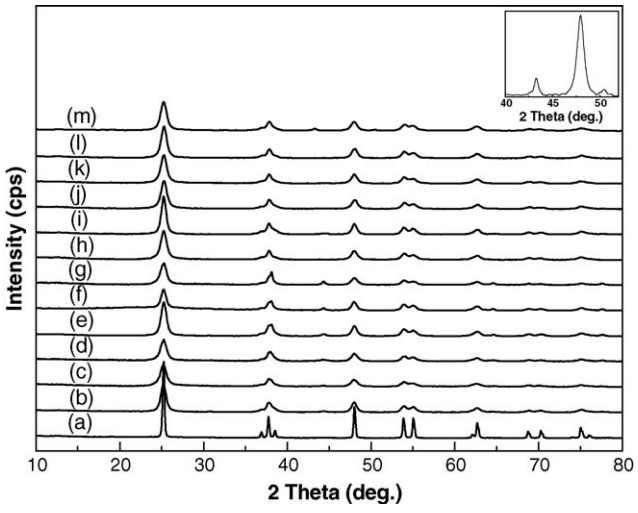

Fig. 1. XRD patterns of all the samples. (*Inset:* Curve is the enlarged XRD pattern of Sample m.)

Table 1
Characteristics of all the samples

Sample	Sample information	Gold content (wt.%)	pH	Anneal atmosphere	Anneal temperature (°C)	Anneal time (h)	Gold size (nm)[a]	$T_{50\%}$ (°C)
a	Au/TiO_2 powder	2	7	Air	300	3	–[b]	188
b	Au/TiO_2 NTs	2	5	Air	300	3	4	95
c	Au/TiO_2 NTs	2	7	Air	200	3	5	106
d	Au/TiO_2 NTs	2	7	Air	300	3	6	47
e	Au/TiO_2 NTs	2	7	Air	400	3	9	82
f	Au/TiO_2 NTs	2	8	Air	300	3	11	75
g	Au/TiO_2 NTs	2	10	Air	300	3	17	116
h	Au/TiO_2 NTs	1	7	Air	300	3	–	54
i	Au/TiO_2 NTs	2	7	H_2	150	2	–	♦[c]
j	Au/TiO_2 NTs	1	7	H_2	150	2	–	♦
k	Au/TiO_2 NTs	0.5	7	H_2	150	2	–	55
l	Au/TiO_2 NTs	0.1	7	H_2	150	2	–	115
m	$Au–Cu/TiO_2$ NTs	0.1	7	H_2	150	2	–	64
n	Cu/TiO_2 NTs	\[d]	\	H_2	150	2	\	74

[a] From line broadening of gold(2 0 0) peak.
[b] No obvious gold peak is observed.
[c] Below room temperature.
[d] Inexistence.

3.2. TEM images of Au/TiO_2 NTs

A deep insight into the system nanostructure can be obtained by TEM observations. Fig. 2 displays TEM images of Sample d at different area. The nanotubes are open-ended, and their diameters are nearly uniform, similar to the results reported by Kasuga et al. [28]. The wall numbers on both sides of the same nanotube are different, which implies that TiO_2 nanotubes are constructed through scrolling the TiO_2 layer sheet [35]. As shown in Fig. 2A, some particles with size less than 3 nm are well-distributed on the multilayer nanotubes. During the deposition–precipitation process, TiO_2 nanotubes act as supports to adsorb gold precursors because of their large surface area. As the gold precursors assemble onto the TiO_2 nanotubes, their aggregation tendency is also prevented. Then small gold particles can be easily obtained after calcination process. Some particles as large as 10 nm are also observed, which are shown in Fig. 2B. It is mainly attributed to the hasty gold deposition during the pH adjustment process. Unlike TEM, particle size comes from XRD is a mean value. Average size of gold particles in Sample d calculated from the X-ray line broadening is 6 nm. Therefore, to get small gold particles that are well-distributed, the deposition process should be precisely controlled.

Fig. 3 shows TEM (A) and HRTEM (B) images of Sample j. It can be observed that large particles are supported on nanoribbons. Fig. 3B shows HRTEM picture of the supported catalysts. Fringes periodicity of the particle is measured as 0.353 nm, consistent well with the lattice spacing between {1 0 1} planes of anatase TiO_2 crystal. No obvious nanotube is observed in the images. It seems that TiO_2 nanotubes are broken after the anneal process in hydrogen gas. And black particles with size less than 5 nm (marked with arrow) should be gold. Compared with the ones that are calcined in air, morphology of the TiO_2 nanotubes can be easily destroyed at lower temperature in hydrogen gas. To validate the conclusions above, pure TiO_2 nanotubes is calcined at 150 °C for 2 h in hydrogen gas. Fig. 4 shows images of the calcined nanotubes. Materials in thorn shape are observed in Fig. 4A. At higher magnification (Fig. 4B), particles with size about 10 nm are observed supported on the bundle of nanoribbons. Obviously, the TiO_2 nanotubes have broken. It has been reported that the TiO_2 nanotubes are composed of corrugated ribbons of edge-sharing TiO_6 octahedra [35,36]. Because of the high surface energy and activity of TiO_2 nanotubes, some unsaturated O can combine with H during the anneal process in hydrogen gas, which may result in the break of Ti–O bonds. As a result, the structure of nanotube is destroyed, and TiO_2

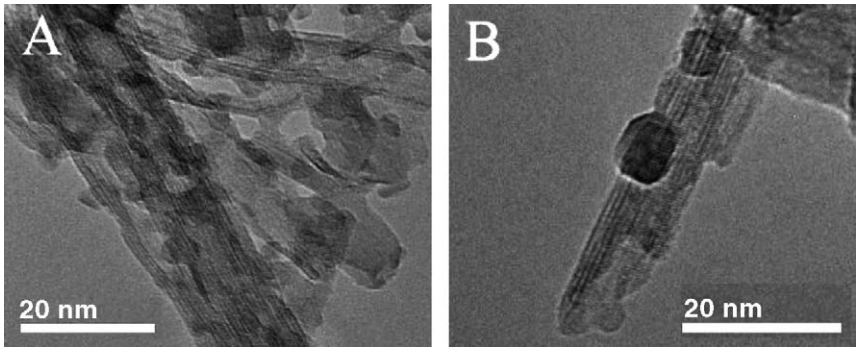

Fig. 2. (A and B) TEM images of Sample d at deferent area.

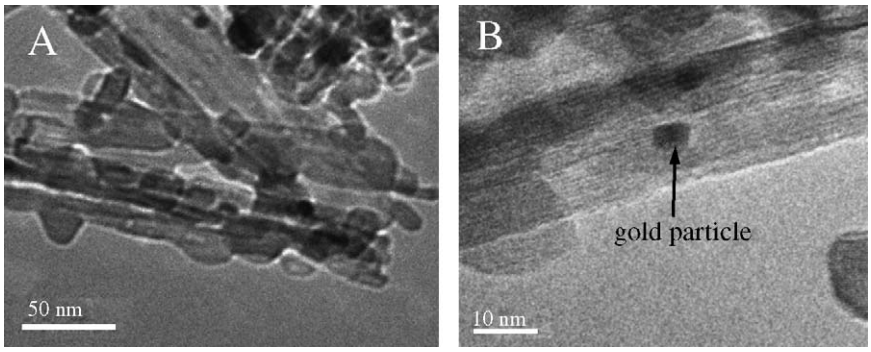

Fig. 3. TEM (A) and HRTEM (B) images of Sample j.

sheets and ribbons form. When the precursor of Au/TiO_2 NTs is calcined in hydrogen gas, gold particles are formed while TiO_2 nanotubes are broken. The broken support prevents the formed gold particles from agglomerating at the same time. It has been reported that the texture of TiO_2 nanotubes can withstand calcination below 400 °C in air [33]. However, our results reveal that the TiO_2 nantubes are easily broken when heated in hydrogen gas.

3.3. Catalytic activity for CO oxidation of the prepared catalysts

3.3.1. Effect of the support

Au/TiO_2 powder and Au/TiO_2 NTs all show catalytic activity for CO oxidation while pure TiO_2 powder and TiO_2 nanotubes exhibit no activity under the same condition. It indicates that gold particles are active centers of the catalysts. Fig. 5 shows the catalytic performance of Samples a and d. CO conversion increases with the raise of reaction temperature for the two catalysts. And catalytic activity of Au/TiO_2 NTs is much higher than that of Au/TiO_2 powder, which is clearly a fact that the form of support has great influence on the activity of Au/TiO_2. It has been reported that catalytic activity of supported gold results from the interaction between gold and support [26]. During the process of catalytic reaction, carbon monoxide and oxygen adhere to gold particles and vacancy sites of TiO_2, respectively. Then the adsorbed oxygen spills on the gold surface and CO turns into CO_2 [37]. The support's propensity for facile adsorption and storage of oxygen, and the high dispersion of gold particles on support play an important role in activating oxygen and CO. Accordingly, catalytic performance of Au/TiO_2 catalysts depends markedly on the support' structure. Compared with TiO_2 powder, TiO_2 nanotubes have larger adsorption capacity for oxygen because of their larger surface area. The spillover process can take place easily and efficiently on Au/TiO_2 NTs as gold particles are highly dispersed on TiO_2 nanotubes. Therefore, Au/TiO_2 NTs shows better catalytic performance for low-temperature CO oxidation.

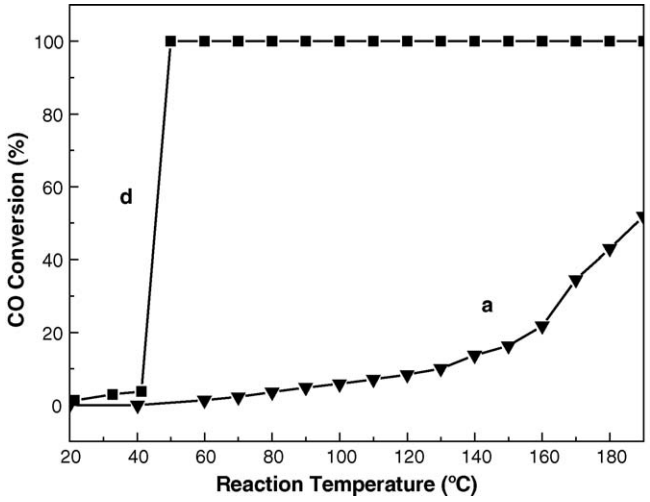

Fig. 5. Catalytic activities of gold-modified catalysts as a function of support form (Sample a, Au/TiO_2 powder; Sample d, Au/TiO_2 NTs).

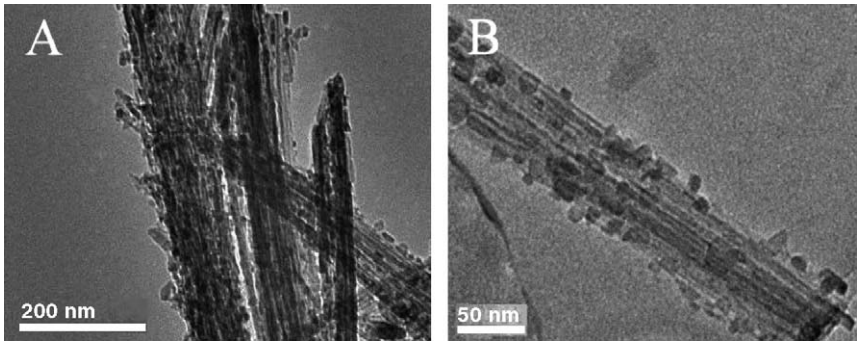

Fig. 4. (A and B) TEM images of TiO_2 nanotubes that are calcined at 150 °C in hydrogen gas.

3.3.2. Effect of the pH of $HAuCl_4$ solution

Fig. 6 shows the catalytic performance of Samples b, d, f and g, which are prepared at different pH of $HAuCl_4$ solution. It reveals that the pH of $HAuCl_4$ solution makes a great influence on the catalytic activity of Au/TiO_2 NTs. The light-off temperature for 100% CO conversion on Samples b, d and f are 130, 50 and 160 °C, respectively. Au/TiO_2 NTs that are prepared at pH 7 (Sample d) have the highest catalytic activity, while the maximal CO conversion on Sample g is 97% under the given reaction condition.

As shown in Table 1, the size of gold particles increases obviously from pH 7 to 10, which may result in the decrease of catalytic activity [13,14]. It is verified by the increase of $T_{50\%}$. Though gold particles obtained at pH 5 (Sample b) are smaller than that are obtained at pH 7 or 8 (Samples d and f), $T_{50\%}$ of Sample b is still higher than that of Samples d and f. It should be attributed to the presence of chloride ions, which is known to be detrimental on activity of the catalyst [38–40]. Haruta has reported that the main species of Au in solution is transformed from $AuCl_4^-$ to $Au(OH)_nCl_{4-n}^-$ ($n = 1$–3) at above pH 6 [25]. At pH 5, large amounts of chlorine ions associate with the gold complex ions that are adsorbed on the support, while more OH^--containing complexes is deposited on TiO_2 nanotubes at higher pH. So, pH 7 is selected to prepare other samples.

3.3.3. Effect of the anneal temperature and atmosphere

Calcination is an indispensable process for preparing Au/TiO_2 NTs catalyst. After anneal process in air or hydrogen atmosphere, Au/TiO_2 NTs are obtained. According to Haruta et al. [41], the calcination process is necessary to form metallic gold particles, which interact with the metal oxide support. The higher the calcination temperature, the stronger interaction exists between gold particles and support. Catalytic property of titania-supported noble metals is associated with the strong metal–support interaction (SMSI) [42]. Agglomeration of gold particles also takes place during the calcination process. Distinct difference in catalytic performance for CO oxidation emerges due to the different treatment processes. CO oxidation performance of Samples c, d and e, which are calcined at various temperatures, are shown in Fig. 7. Catalytic activity of Sample h is also included in this figure. It can be seen that the effect of anneal temperature is quite distinct. Though small gold particles can be obtained at low temperature, interaction between gold and TiO_2 nanotubes is rather weak. On the other hand, calcination at high temperature accelerates the agglomeration of gold particles and decreases the activity of catalysts. For 2 wt.% Au/TiO_2 NTs calcined in air, the Sample d, which is calcined at 300 °C, has the best catalytic performance. It means that 300 °C should be the appropriate anneal temperature in air.

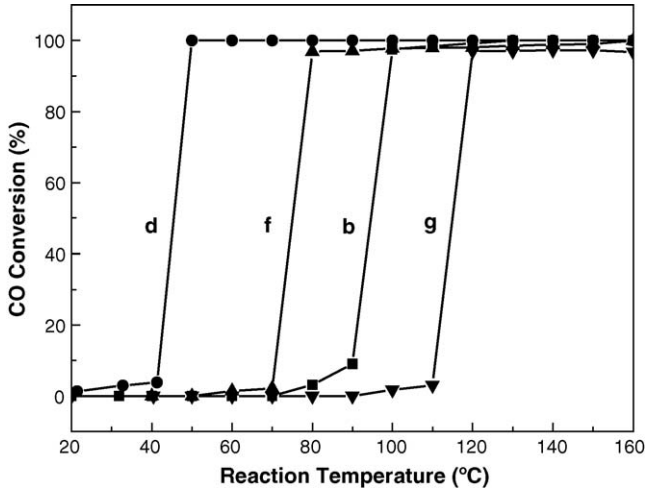

Fig. 6. Catalytic activities of Au/TiO_2 NTs as a function of pH adjustment (Sample b, pH 5; Sample d, pH 7; Sample f, pH 8; Sample g, pH 10).

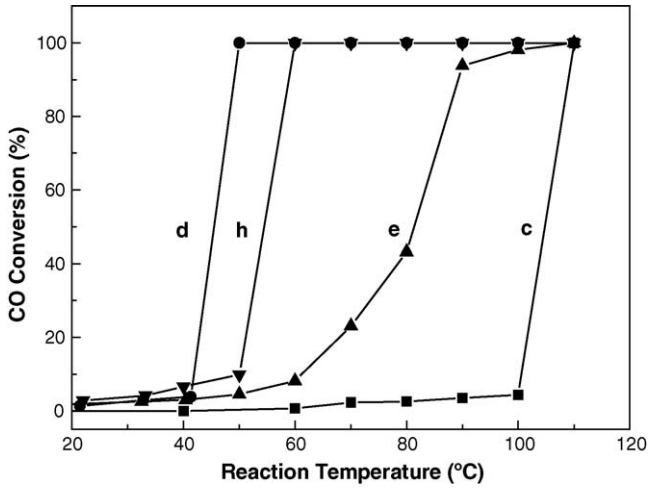

Fig. 7. Catalytic activities of Au/TiO_2 NTs as a function of anneal temperature (Sample c, 2 wt.% Au, calcined at 200 °C; Sample d, 2 wt.% Au, calcined at 300 °C; Sample e, 2 wt.% Au, calcined at 400 °C; Sample h, 1 wt.% Au, calcined at 300 °C).

Calcination in hydrogen atmosphere results in better catalytic performance. For 2 and 1 wt.% Au/TiO_2 NTs that are calcined in hydrogen gas (Samples i and j), their $T_{100\%}$ are below room temperature, while $T_{100\%}$ of samples heated at 300 °C in air (Samples d and h) are 60 and 50 °C, respectively. As has been discussed above, morphology of the TiO_2 nanotubes is destroyed after the calcination process in hydrogen. However, the break of TiO_2 nanotubes also prevent the agglomeration of gold particles and small gold particles form finally. It has been reported that size of gold particles have considerably more influence than the form of support on catalytic activity of supported gold for CO oxidation [10]. So, supported gold catalyst with higher activity for CO oxidation can be prepared after calcination process in hydrogen gas.

3.3.4. Effect of the gold content and copper doping

2 wt.% Au/TiO_2 NTs have higher catalytic activity than the 1 wt.% ones, which can be seen in Table 1. Fig. 8 shows the catalytic performance of Samples k, l, m and n. For 1 wt.% Au/TiO_2 NTs (Sample j), its $T_{100\%}$ is below room temperature. However, the $T_{100\%}$ of 0.5 wt.% (Sample k) and 0.1 wt.% Au/TiO_2 NTs (Sample l) are 60 and 170 °C, respectively. Obviously, the conversion of CO rises with the increase of gold content. Using copper-modified TiO_2 nanotubes as support, catalytic activity of supported gold can be enhanced greatly. Compared with the

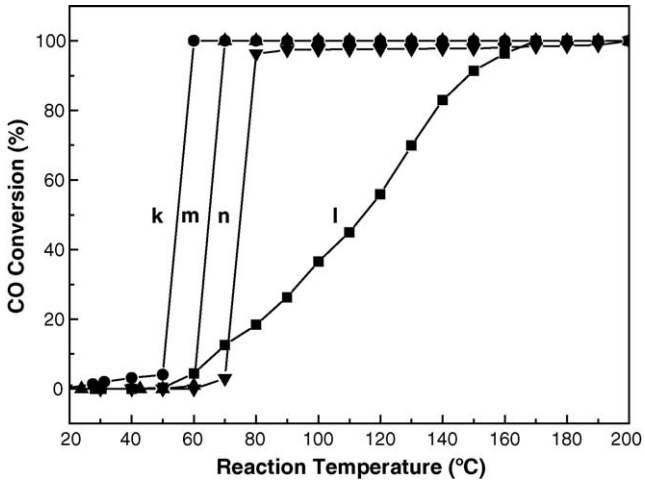

Fig. 8. Catalytic activities of gold-modified catalysts as a function of gold content and copper doping (Sample k, 0.5 wt.% Au; Sample l, 0.1 wt.% Au; Sample m, Au–Cu/TiO_2 NTs; Sample n, Cu/TiO_2 NTs).

Au/TiO_2 NTs with low gold content, Au–Cu/TiO_2 NTs possess higher activity. $T_{100\%}$ of Sample m is 70 °C, which is 100 °C lower than that of Sample l. Catalytic performance of Sample n is also presented in Fig. 8 for comparative study. Though its light-off temperature for CO oxidation is 80 °C, 100% CO conversion cannot be obtained until 200 °C on it. There should be a synergistic interaction between gold and copper, which is responsible for the high activity. It is distinct that cheap copper can replace part of gold. Rather than to decrease the activity of catalysts, adding copper even increases the activity. It enables the replacement of a high gold loading catalyst with a lower gold loading catalyst in order to achieve the same conversion. From the view of economic factors, it is a favor in using low gold content for supported catalyst.

The CO oxidation activities of Samples j and m as a function of reaction time are also monitored. After 100% CO conversion is obtained on them, the CO conversion is measured every half an hour under the same experiment condition ($T = T_{100\%}$). Activities of the catalysts do not decay over 10 h in the present study, which indicates high stability of the prepared catalysts.

4. Conclusions

In this work, Au/TiO_2 powder, Au/TiO_2 NTs and Au–Cu/TiO_2 NTs are fabricated by deposition–precipitation method. Catalytic performance of these catalysts depends markedly on the form of support and high catalytic activity can be obtained by using TiO_2 nanotubes as support. Besides, the catalytic activity of Au/TiO_2 NTs strongly depends on pH of $HAuCl_4$ solution, calcination temperature and atmosphere, and gold content. An exact control of experimental conditions is very important to prepare Au/TiO_2 NTs with high activity. It should be pointed out that gold particles form while the TiO_2 nanotubes are broken when the gold precursor-loaded TiO_2 nanotubes are calcined in hydrogen gas. Small gold particles and high catalytic activity are obtained as a result. Compared with Au/TiO_2 NTs, Au–Cu/TiO_2 NTs show better catalytic performance. This is a significative attempt for TiO_2 nanotubes as catalyst carriers.

Acknowledgment

This work is supported by 973 Program (2005CB623607).

References

[1] N.W. Cant, N.J. Ossipoff, Catal. Today 36 (1997) 125–133.
[2] A.K. Santra, D.W. Goodman, Electrochim. Acta 47 (2002) 3595–3609.
[3] H.Q. Zhu, Z.F. Qin, W.J. Shan, W.J. Shen, J.G. Wang, J. Catal. 233 (2005) 41–50.
[4] X.C. Zheng, S.H. Wu, S.P. Wang, S.R. Wang, S.M. Zhang, W.P. Huang, Appl. Catal. A 283 (2005) 217–223.
[5] M. Haruta, T. Kobayashi, H. Sano, N. Yamada, Chem. Lett. 2 (1987) 405–408.
[6] M. Haruta, N. Yamada, T. Kobayashi, S. Iijima, J. Catal. 115 (1989) 301–309.
[7] Y.Z. Yuan, A.P. Kozlova, K. Asakura, H.L. Wan, K. Tsai, Y. Iwasawa, J. Catal. 170 (1997) 191–199.
[8] A.I. Kozlov, A.P. Kozlova, H. Liu, Y. Iwasawa, Appl. Catal. A 182 (1999) 9–28.
[9] M. Maciejewski, P. Fabrizioli, J.D. Grunwaldt, O.S. Becker, A. Baiker, Phys. Chem. Chem. Phys. 3 (2001) 3846–3855.
[10] N. Lopez, T.V.W. Janssens, B.S. Clausen, Y. Xu, M. Mavrikakis, T. Bligaard, J.K. Nørskov, J. Catal. 223 (2004) 232–235.
[11] M.M. Schubert, S. Hackenberg, A.C.V. Veen, M. Muhler, V. Plzak, R.J. Behm, J. Catal. 197 (2001) 113–122.
[12] S. Arrii, F. Morfin, A.J. Renouprez, J.L. Rousset, J. Am. Chem. Soc. 126 (2004) 1199–1205.
[13] F. Boccuzzi, A. Chiorino, M. Manzoli, Mater. Sci. Eng. C 15 (2001) 215–217.
[14] D.C. Meier, D.W. Goodman, J. Am. Chem. Soc. 126 (2004) 1892–1899.
[15] P. Konova, A. Naydenov, C. Venkov, D. Mehandjiev, D. Andreeva, T. Tabakova, J. Mol. Catal. A 213 (2004) 235–240.
[16] J.D. Stiehl, T.S. Kim, S.M. McClure, C.B. Mullins, J. Phys. Chem. B 109 (2005) 6316–6322.
[17] A.M. Visco, F. Neri, G. Neri, A. Donato, C. Milone, S. Galvagno, Phys. Chem. Chem. Phys. 1 (1999) 2869–2873.
[18] N.A. Hodge, C.J. Kiely, R. Whyman, M.R.H. Siddiqui, G.J. Hutchings, Q.A. Pankhurst, F.E. Wagner, R.R. Rajaram, S.E. Golunski, Catal. Today 72 (2002) 133–144.
[19] M.M. Schubert, A. Venugopal, M.J. Kahlich, V. Plzak, R.J. Behm, J. Catal. 222 (2004) 32–40.
[20] M. Manzoli, A. Chiorino, F. Boccuzzi, Appl. Catal. B 52 (2004) 259–266.
[21] G.Y. Wang, W.X. Zhang, H.L. Lian, D.Z. Jiang, T.H. Wu, Appl. Catal. A 239 (2003) 1–10.
[22] G. Panzera, V. Modafferi, S. Candamano, A. Donato, F. Frusteri, P.L. Antonucci, J. Power Sources 135 (2004) 177–183.
[23] P.X. Huang, F. Wu, B.L. Zhu, X.P. Gao, H.Y. Zhu, T.Y. Yan, W.P. Huang, S.H. Wu, D.Y. Song, J. Phys. Chem. B 109 (2005) 19169–19174.
[24] A. Wolf, F. Schüth, Appl. Catal. A 226 (2002) 1–13.
[25] M. Haruta, A. Ueda, S. Tsubota, R.M.T. Sanchez, Catal. Today 29 (1996) 443–447.
[26] M.M. Schubert, V. Plzak, J. Garche, R.J. Behm, Catal. Lett. 76 (2001) 143–150.
[27] X. Liu, T.F. Jaramillo, A. Kolmakov, S.H. Baeck, M. Moskovits, G.D. Stucky, E.W. McFarland, J. Mater. Res. 20 (2005) 1093–1096.
[28] T. Kasuga, M. Hiramatsu, A. Hoson, T. Sekino, K. Niihara, Langmuir 14 (1998) 3160–3163.
[29] B.D. Yao, Y.F. Chan, X.Y. Zhang, W.F. Zhang, Z.Y. Yang, N. Wang, Appl. Phys. Lett. 82 (2003) 281–283.
[30] V. Idakiev, Z.Y. Yuan, T. Tabakova, B.L. Su, Appl. Catal. A 281 (2005) 149–155.

[31] T. Akita, M. Okumura, K. Tanaka, K. Ohkuma, M. Kohyama, T. Koyanagi, M. Date, S. Tsubota, M. Haruta, Surf. Interface Anal. 37 (2005) 265–269.
[32] B.L. Zhu, Z.M. Sui, X. Chen, S.R. Wang, S.M. Zhang, S.H. Wu, W.P. Huang, Chin. Sci. Bull. 50 (2005) 711–713.
[33] M. Zhang, Z.S. Jin, J.W. Zhang, X.Y. Guo, J.J. Yang, W. Li, X.D. Wang, Z.J. Zhang, J. Mol. Catal. A 217 (2004) 203–210.
[34] H.P. Klug, L.E. Alexander, X-Ray Diffraction Procedures, second ed., Wiley, New York, 1974.
[35] R. Ma, Y. Bando, T. Sasaki, Chem. Phys. Lett. 380 (2003) 577–582.
[36] Q. Chen, W.Z. Zhou, G.H. Du, L.M. Peng, Adv. Mater. 14 (17) (2002) 1208–1211.
[37] J.D. Grunwaldt, A. Baiker, J. Phys. Chem. B 103 (1999) 1002–1012.
[38] F. Moreau, G.C. Bond, A.O. Taylor, Chem. Commun. (2004) 1642–1643.
[39] H.H. Kung, M.C. Kung, C.K. Costello, J. Catal. 216 (2003) 425–432.
[40] M.A. Bollinger, M.A. Vannice, Appl. Catal. B 8 (1996) 417–443.
[41] M. Haruta, S. Tsubota, T. Kobayashi, H. Kageyama, M.J. Genet, B. Delmon, J. Catal. 144 (1993) 175–192.
[42] K.I. Hadjiivanov, D.G. Klissurski, Chem. Soc. Rev. 25 (1996) 61–69.